International Scholarly Research Network
ISRN Spectroscopy
Volume 2012, Article ID 639041, 6 pages
doi:10.5402/2012/639041

Research Article

Effect of Annealing on Optical Properties of $ZnO \cdot LiF \cdot B_2O_3$ Glasses

Susheel Arora,[1] Virender Kundu,[2] D. R. Goyal,[1] and A. S. Maan[1]

[1] *Department of Physics, Maharshi Dayanand University, Rohtak 124 001, India*
[2] *Electronic Science Department, Kurukshetra University, Kurukshetra 136119, India*

Correspondence should be addressed to Susheel Arora, susheel_arora@yahoo.com

Received 9 August 2012; Accepted 17 September 2012

Academic Editors: J. Casado, J.-H. Choi, and A. Polimeni

The Melt-quench method is used to synthesize zinc fluoroborate glasses with compositions $x\text{ZnO} \cdot (40 - x)\text{LiF} \cdot 60\text{B}_2\text{O}_3$ ($x = 0$, 5, 10, 15, and 20). Optical characterization was carried out to examine the variation of optical bandgap energy (E_g) and urbach energy (E_U) with respect to the concentration for the samples annealed at different temperatures (300°C, 350°C, and 400°C). Annealing shows its effect on the samples with the variations in the values of E_g and E_U. These variations are explained on the basis of formation of different molecular species like BO_3^- units, boroxol rings, and the change in the number of nonbridging oxygen atoms.

1. Introduction

Crystallization of a melt can be avoided by a sufficient fast cooling rate to form the amorphous phase. In borate glasses, boron-oxygen triangles bear sheet like structure with their ability to connect themselves to form a network. This characteristic has popularized B_2O_3 as one of the best glass formers [1, 2]. The requirement of random arrangement of various atomic and molecular species is easily fulfilled in borate glasses. With the addition of alkali halides in borate glasses there appears modifications in some properties of these glasses due to variations that occurred in their structures [3–9]. These modifications are reported for the inclusion of LiF in the borate glasses [3]. Some oxygen atoms get replaced by fluorine ions in the network to form new units like BO_2F, BO_2F_2, BOF_3, and BO_3F [4–6]. There may be an increase in the number of nonbridging oxygen atoms due to the increase in polyhedral groups of boron and oxygen [7–9]. Modifications in microstructure of a substance are observed in terms of variations of various properties like optical, physical, electrical and structural, and so forth. Structure and therefore optical characteristics of a material are affected by nonhomogeneous cooling of the melt. The effect of annealing at different temperatures on optical and structural properties of B_2O_3 glasses is reported so far [10–14]. In these glasses, there is always a possibility of formation of B_3O_6 rings called boroxol rings, by the combination of BO_3 groups. Raman spectroscopy reveals that for annealing temperature greater than the glass transition temperature, the concentration of boroxol rings increases with a decrease in temperature [13]. There appears a residual stress in such materials. During annealing of a glass, a thermodynamical and mechanical steady state is achieved after a specific time and temperature.

This paper reports the effect of annealing at different temperatures on optical properties of $\text{ZnO} \cdot \text{LiF} \cdot \text{B}_2\text{O}_3$ glasses. With the addition of ZnO new molecular units are expected to be formed which affects the glass structure by changing the number of NBOs. Due to this reason optical bandgap energy and urbach energy change with composition.

2. Experimental Details

2.1. Sample Preparation. Fluoroborate glasses containing ZnO with compositions $x\text{ZnO} \cdot (40 - x)\text{LiF} \cdot 60\text{B}_2\text{O}_3$ ($x = 0, 5, 10, 15$, and 20) glasses were synthesized through melt-quench method using ZnO, LiF, and H_3BO_3, reagent grade

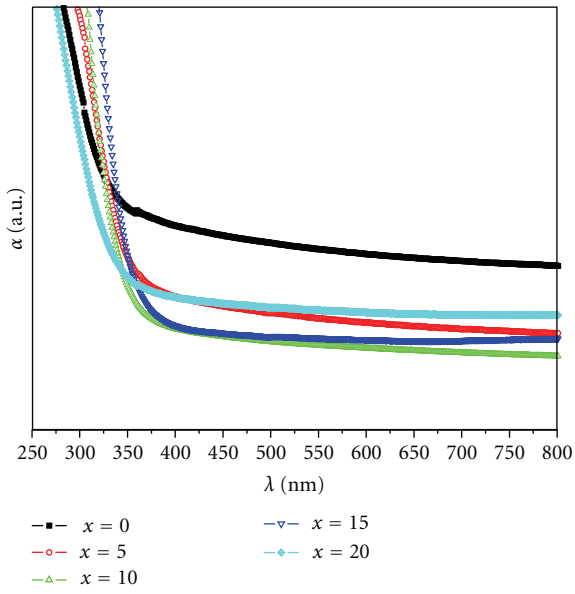

Figure 1: Optical absorption coefficient versus wavelength plots for samples annealed at 300°C with $x = 0, 5, 10, 15$, and 20 in the compositions $x\text{ZnO}\cdot(40 - x)\text{LiF}\cdot 60\text{B}_2\text{O}_3$.

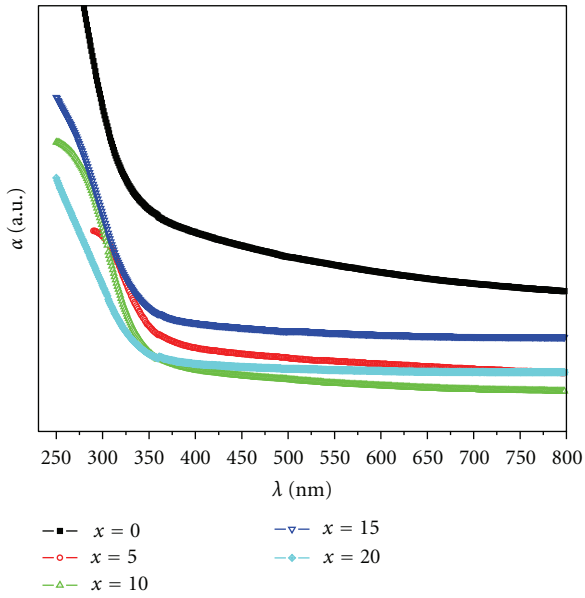

Figure 2: Optical absorption coefficient versus wavelength plots for samples annealed at 350°C with $x = 0, 5, 10, 15$, and 20 in the compositions $x\text{ZnO}\cdot(40 - x)\text{LiF}\cdot 60\text{B}_2\text{O}_3$.

powders. Various powdered materials were taken in grams equal to their molecular masses and were mixed uniformly according to their percentage presence in various samples. The uniform mixture was heated at 1273 K for 30 minutes. The bubble-free melt formed was pressed between two carbon plates at room temperature. The glassy samples were thus obtained in the form of thin pallets with an average thickness of 1 mm each.

2.2. Annealing. Samples were annealed at 300°C, 350°C, and 400°C for 2 hrs each. The samples obtained were then tested for optical properties.

2.3. Optical Characterization. Optical characterization was carried out in the wavelength range 200–1000 nm using Perkin-Elmer UV-Visible spectrophotometer at room temperature. Plots between the absorption and wavelength of incident radiations were obtained for further analysis.

3. Results and Discussion

3.1. Optical Analysis. A series of samples in $x\text{ZnO}\cdot(40 - x)\text{LiF}\cdot 60\text{B}_2\text{O}_3$ compositions with $x = 0, 5, 10, 15$, and 20 annealed at temperatures 300°C, 350°C, and 400°C are tested for UV-visible absorption at room temperature. The absorption profiles of annealed samples are depicted in Figures 1, 2, and 3, which are the plots of absorption coefficient $\alpha(\nu)$ versus wavelength of incident radiation.

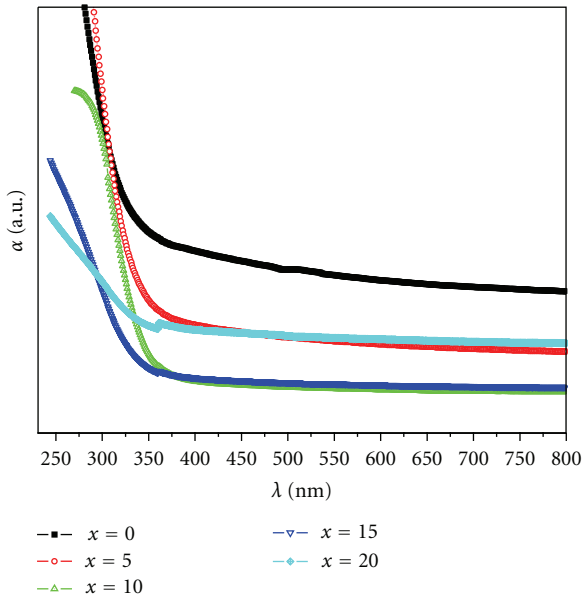

Figure 3: Optical absorption coefficient versus wavelength plots for samples annealed at 400°C with $x = 0, 5, 10, 15$, and 20 in the compositions $x\text{ZnO}\cdot(40 - x)\text{LiF}\cdot 60\text{B}_2\text{O}_3$.

The absorption coefficient $\alpha(\nu)$ is related to transmitted intensity (I_t), incident intensity (I_i), and the thickness of the sample (t) [15] as

$$\alpha(\nu) = \left(\frac{1}{t}\right)\ln\left(\frac{I_i}{I_t}\right). \quad (1)$$

Absence of sharp absorption edge in all the plots given in Figures 1, 2, and 3 confirms that the samples are amorphous

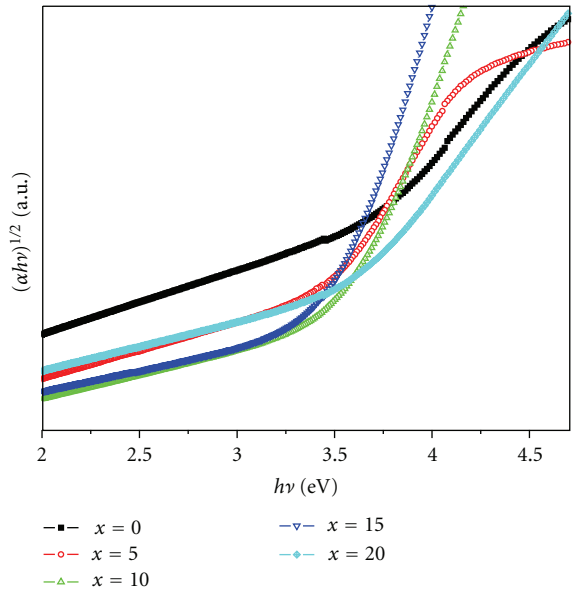

Figure 4: Tauc's plots with $r = 2$ for samples annealed at 300°C with $x = 0, 5, 10, 15$, and 20 in the compositions xZnO·(40 − x)LiF·60B_2O_3.

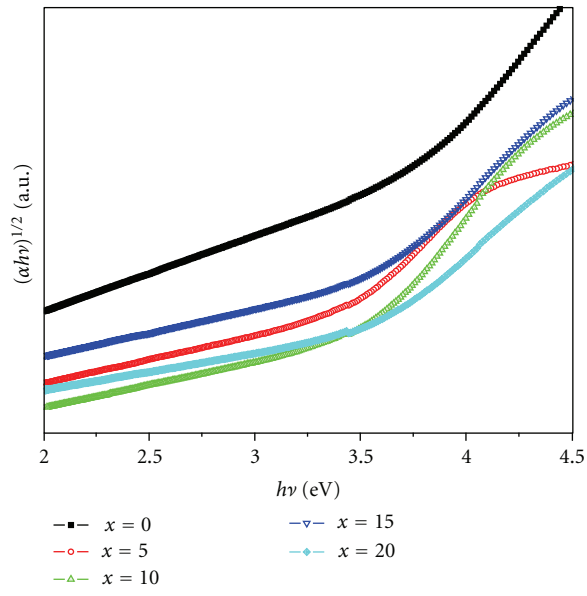

Figure 5: Tauc's plots with $r = 2$ for samples annealed at 350°C with $x = 0, 5, 10, 15$, and 20 in the compositions xZnO·(40 − x)LiF·60B_2O_3.

in nature. Optical bandgap energy is an important parameter which reflects the optical behavior of a sample in terms of its transparency towards electromagnetic radiations. The optical bandgap energy (E_g) is related to the absorption coefficient $\alpha(\nu)$ [15] as

$$\alpha h\nu = B\left(h\nu - E_g\right)^r. \quad (2)$$

In this equation ν is the frequency of incident radiation and B is a constant named as band tailing parameter. The value of the index r suggests the nature of transitions taking place in the sample. For indirect allowed and forbidden transitions r equals 2 and 3, respectively, and for direct allowed and forbidden transitions r equals 1/2 and 2/3, respectively. Tauc's plots $[(\alpha h\nu)^{1/r}$ versus $h\nu, r = 2]$ for the reported samples are shown in Figures 4, 5, and 6. Values of optical bandgap energy E_g are obtained by extrapolating the linear regions of Tauc's plots. The variation of E_g against the composition for the samples annealed at different temperatures is listed in Table 1 and plotted in Figure 7.

At annealing temperature 300°C, optical bandgap energy increases from $x = 0$ to $x = 10$ with maximum at $x = 10$ and then decreases for $x = 15$ and $x = 20$. This trend is followed for the annealing temperature 350°C with a decreased value of E_g for each sample. It is expected here that during annealing of the samples at 350°C, some of BO_4 structural units get converted in BO_3^- units with one nonbridging oxygen atom (NBO) each. Therefore an increase in the number of NBOs decreases the value of E_g. For annealing temperature 400°C there is a change in optical behavior of the samples. In this case the value of E_g increases for the samples with $x = 0$ to $x = 15$ and decreases for the sample with $x = 20$ as compared to its value at annealing temperature 350°C. It is expected that in the samples with

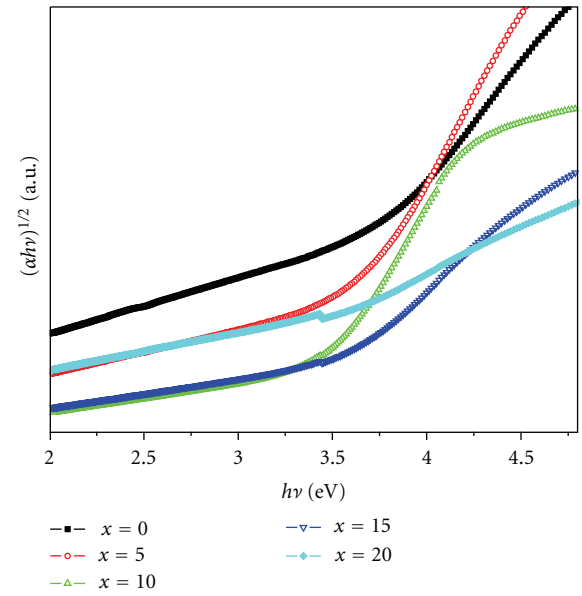

Figure 6: Tauc's plots with $r = 2$ for samples annealed at 400°C with $x = 0, 5, 10, 15$, and 20 in the compositions xZnO·(40 − x)LiF·60B_2O_3.

$x = 0$ to $x = 15$ BO_3 units get connected to themselves to form boroxol rings. This phenomenon results in a decrease in the number of NBOs and in turn an increase in the optical bandgap energy. For the sample with $x = 20$ the formation of BO_3^- units from BO_4 units dominates over the phenomenon of the formation of boroxol rings, which results in a decrease in the value of E_g. Although, the trend of variation of E_g in

Table 1: Cutoff wavelength (λ_{cutoff}), optical band gap energy E_g, and Urbach energy (E_U) for the samples with $x = 0, 5, 10, 15$, and 20 in the compositions xZnO·$(40 - x)$LiF·60 B_2O_3.

Annealing temperature (°C)	x (mol%)	λ_{cutoff} (nm)	E_g (eV)	B (cm eV)$^{-1}$	E_U (eV)
300	0	375	2.85	1.3234	0.9325
	5	371	3.13	3.0002	0.4877
	10	350	3.42	8.4344	0.3443
	15	356	3.35	12.1620	0.3249
	20	360	3.10	1.7609	0.6249
350	0	366	2.80	1.5250	1.2799
	5	391	2.95	1.0723	0.8693
	10	356	3.23	1.6381	0.6494
	15	372	2.91	1.1500	1.0000
	20	375	2.90	0.7557	1.0724
400	0	356	3.00	1.7609	1.1504
	5	344	3.25	3.5370	0.7002
	10	350	3.30	3.0001	0.5095
	15	357	3.19	0.8700	0.8391
	20	426	2.45	0.2600	1.7319

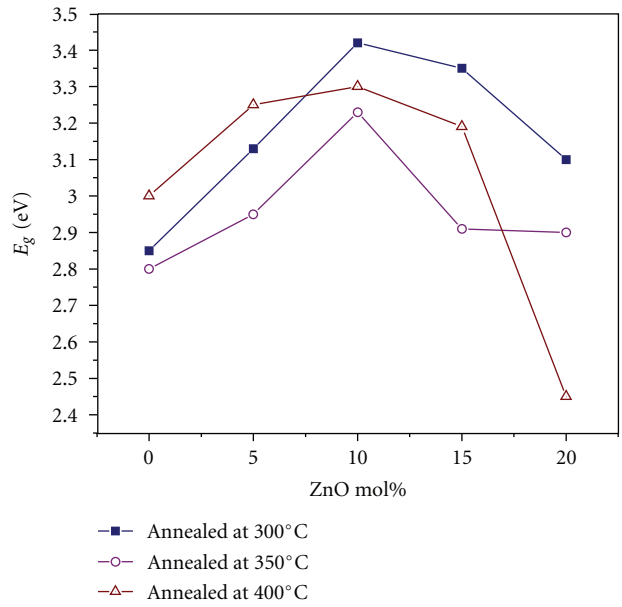

Figure 7: Variation of E_g with composition for samples with $x = 0$, 5, 10, 15, and 20 in the compositions xZnO·$(40 - x)$LiF·60B_2O_3.

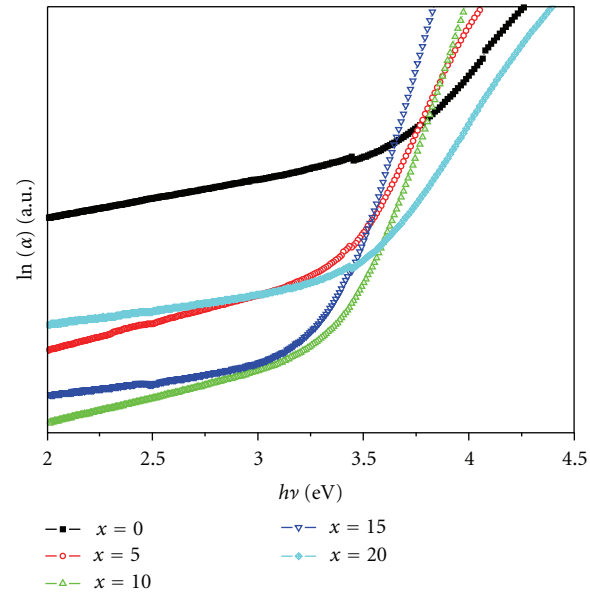

Figure 8: Urbach plots for samples annealed at 300°C with $x = 0, 5, 10, 15$, and 20 in the compositions xZnO·$(40 - x)$LiF·60B_2O_3.

annealed samples remains almost the same with respect to concentration for all annealing temperatures.

In the low absorption region of Tauc's plot the absorption coefficient is related to photon energy [16] as

$$\alpha \sim \exp\left(\frac{h\nu}{E_U}\right). \quad (3)$$

Here E_U is named as urbach tail energy which corresponds to the width of the tail states in the mobility gap. Disordered arrangement of atoms causes the mobility edges to enter in the mobility gap and give rise to the tail states. The formation of such localized states can thus be attributed to the random potential fluctuations [17]. The electronic transitions taking place in such states are generally phonon assisted [18, 19]. The formation of such states in the materials makes it the indirect bandgap material. Therefore, one can conclude that the reported samples are the indirect bandgap materials.

The value of E_U for the reported samples is calculated from the inversus of the slopes of the linear parts of the urbach plots (ln$\alpha\nu$/$sh\nu$), shown in Figures 8, 9, and 10. The values of E_U for samples annealed at different temperatures are listed in Table 1 and the variation of E_U is plotted against the composition in Figure 11.

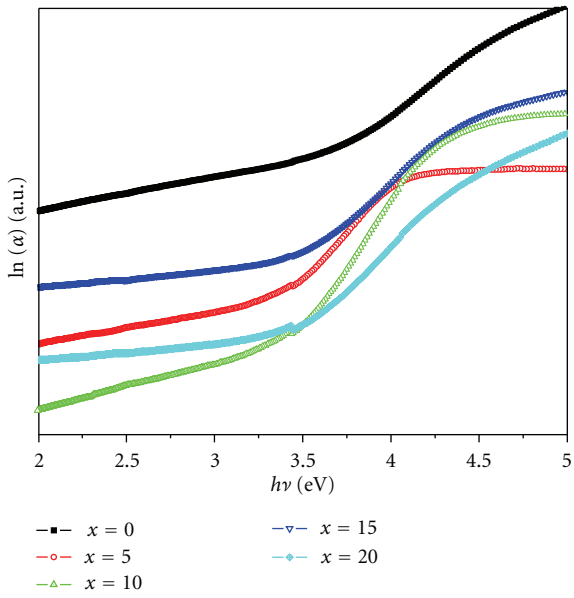

Figure 9: Urbach plots for samples annealed at 350°C with $x = 0, 5, 10, 15$, and 20 in the compositions xZnO·$(40 - x)$LiF·$60B_2O_3$.

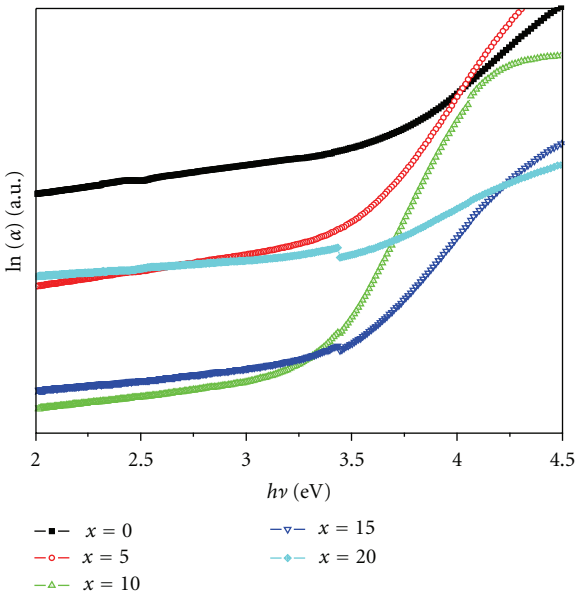

Figure 10: Urbach plots for samples annealed at 400°C with $x = 0, 5, 10, 15$, and 20 in the compositions xZnO·$(40 - x)$LiF·$60B_2O_3$.

At annealing temperature 350°C E_U is more than that at annealing temperature 300°C for all the samples. It again decreases at annealing temperature 400°C as compared to that at annealing temperature 350°C, except for the sample with $x = 20$, which increases remarkably. It can be explained on the same ground that at annealing temperature 350°C more BO_3^- units are formed as compared to those at annealing temperature 300°C and hence the number of NBOs increases. This results in more potential fluctuations

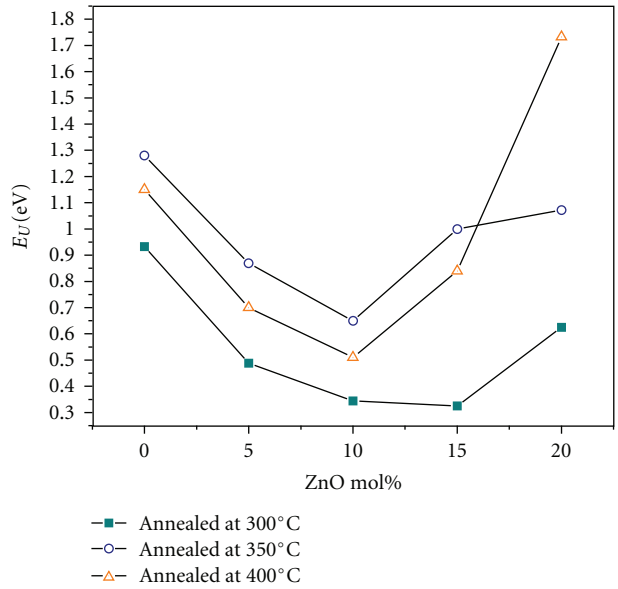

Figure 11: Variation of Urbach tail energy with composition for samples with $x = 0, 5, 10, 15$, and 20 in the compositions xZnO·$(40 - x)$LiF·$60B_2O_3$.

to enter in the mobility gap which increases the value of E_U. At annealing temperature 400°C, the expected formation of boroxol rings decreases the number of NBOs and so the mobility gap fluctuations. Therefore the value of E_U decreases for samples with $x = 0$ to $x = 15$ as compared to their respective values at annealing temperature 350°C. And due to the formation of more BO_3^- units than boroxol rings, E_U increases for the sample with $x = 20$ as compared to its value at annealing temperature 350°C.

4. Conclusions

(1) In the series of samples xZnO·$(40 - x)$LiF·60 B_2O_3, values of E_g at annealing temperature 300°C increase from $x = 0$ to $x = 10$ and decrease for the samples with $x = 15$ and $x = 20$. This trend is followed by all the samples at annealing temperature 350°C with decreased values of E_g, due to the formation of more BO_3^- units. Values of E_U at annealing temperature 350°C are more than those at annealing temperature 300°C for all the samples. This is also due to the same reason as explained above.

(2) At annealing temperature 400°C values of E_g again increase and values of E_U decrease for the samples with $x = 0$ to $x = 15$ as compared to their values at annealing temperature 350°C, due to the formation of boroxol rings. For the sample with $x = 20$ the phenomenon of formation of BO_3^- units dominates over the formation of boroxol rings. Therefore, value of E_g again decreases and that of E_U increases.

References

[1] C. Boussard-Plédel, M. Le Floch, G. Fonteneau et al., "The structure of a boron oxyfluoride glass, an inorganic cross-linked chain polymer," *Journal of Non-Crystalline Solids*, vol. 209, no. 3, pp. 247–256, 1997.

[2] G. D. Chryssikos, M. S. Bitsis, J. A. Kapoutsis, and E. I. Kamitsos, "Vibrational investigation of lithium metaborate-metaaluminate glasses and crystals," *Journal of Non-Crystalline Solids*, vol. 217, no. 2-3, pp. 278–290, 1997.

[3] C. Boussard-Plédel, G. Fonteneau, and J. Lucas, "Boron oxyfluoride glasses in the BOF system: new polymeric spaghetti-type glasses," *Journal of Non-Crystalline Solids*, vol. 188, no. 1-2, pp. 147–152, 1995.

[4] N. Soga, "Elastic moduli and fracture toughness of glass," *Journal of Non-Crystalline Solids*, vol. 73, no. 1–3, pp. 305–313, 1985.

[5] I. Z. Hager, "Elastic moduli of boron oxyfluoride glasses: experimental determinations and application of Makishima and Mackenzie's theory," *Journal of Materials Science*, vol. 37, no. 7, pp. 1309–1313, 2002.

[6] I. Z. Hager and M. El-Hofy, "Investigation of spectral absorption and elastic moduli of lithium haloborate glasses," *Physica Status Solidi (A) Applied Research*, vol. 198, no. 1, pp. 7–17, 2003.

[7] J. E. Shelby and L. K. Downie, "Properties and structure of sodium fluoroborate glasses," *Physics and Chemistry of Glasses*, vol. 30, no. 4, pp. 151–154, 1989.

[8] G. D. Chryssikos, E. I. Kamitsos, A. P. Patsis, M. S. Bitsis, and M. A. Karakassides, "The devitrification of lithium metaborate: polymorphism and glass formation," *Journal of Non-Crystalline Solids*, vol. 126, no. 1-2, pp. 42–51, 1990.

[9] E. I. Kamitsos, A. P. Patsis, and G. D. Chryssikos, "Infrared reflectance investigation of alkali diborate glasses," *Journal of Non-Crystalline Solids*, vol. 152, no. 2-3, pp. 246–257, 1993.

[10] C. Martin, C. Chaumont, J. P. Sanchez, and J. C. Bernier, "Influence of preparation process on physical properties and devitrification of $Li_2B_2O_4$ (0,9) $LiFe_5O_8$ (0,1)glasses," *Journal De Physique Colloques*, vol. 46, no. C8, pp. 585–589, 1985.

[11] H. A. McMaster, "Variations of refractive index of glass with time and temperature in annealing region," *Journal of the American Ceramic Society*, vol. 28, no. 1, p. 1, 1945.

[12] L. W. Tilton, F. W. Rosberry, and F. T. Badger, "Refractive uniformity of a borosilicate glass after different annealing treatments," *Journal of Research of the National Bureau of Standards*, vol. 49, no. 1, pp. 21–32, 1952.

[13] N. V. Surovtsev, J. Wiedersich, A. E. Batalov, V. N. Novikov, M. A. Ramos, and E. Rössler, "Inelastic light scattering in B_2O_3 glasses with different thermal histories," *Journal of Chemical Physics*, vol. 113, no. 14, pp. 5891–5900, 2000.

[14] S. A. Kartha, M. A. Ittyachen, B. Pradeep, and M. Abdul Khadar, "Effect of annealing on the optical properties of B_2O_3-Li_2O-PbO glass thin films," *Journal of Materials Science Letters*, vol. 22, no. 1, pp. 9–11, 2003.

[15] E. A. Devis and N. F. Mott, "Conduction in non-crystalline systems V. Conductivity, optical absorption and photoconductivity in amorphous semiconductors," *Philosophical Magazine*, vol. 22, pp. 0903–0922, 1970.

[16] F. Urbach, "The long-wavelength edge of photographic sensitivity and of the electronic Absorption of Solids," *Physical Review*, vol. 92, no. 5, p. 1324, 1953.

[17] A. A. Kutub, A. E. Mohamed-Osman, and C. A. Hogarth, "Some studies of the optical properties of copper phosphate glasses containing praseodymium," *Journal of Materials Science*, vol. 21, no. 10, pp. 3517–3520, 1986.

[18] C. Dayanand, G. Bhikshamaiah, and M. Salagram, "IR and optical properties of PbO glass containing a small amount of silica," *Materials Letters*, vol. 23, no. 4–6, pp. 309–315, 1995.

[19] K. L. Chopra and S. K. Bahl, "Exponential tail of the optical absorption edge of amorphous semiconductors," *Thin Solid Films*, vol. 11, no. 2, pp. 377–388, 1972.